In situ Electrochemical Fluorescence Studies of PPV

F. Montilla and R. Mallavia*

Instituto de Biología Molecular y Celular, Universidad Miguel Hernández, Avda. de la Universidad s/n, Elche (Alicante), Spain E-03202

Received: August 7, 2006; In Final Form: October 16, 2006

Conjugated phenylene−vinylene polymers are widely used in organic light-emitting and photovoltaic devices. The comprehension of the optical properties upon charge injection is of crucial importance for the improvement of such organoelectronic devices. The processes of electrochemical doping, electrolyte diffusion, and degradation have been studied by cyclic voltammetry and chronoamperometric methods. Kinetic studies by in situ fluorescence spectroscopy have been used for the determination of the mobility of charge carriers in the polymer making used of electrochemical Stern−Volmer analysis. The mobility of holes for MDMO−PPV measured by this method was 2.5×10^{-7} cm^2 V s^{-1}. Non-Faradic variations of the fluorescence after doping−dedoping cycles have been related to morphological changes in the polymeric layer. The evolution of the fluorescence obeys a first-order kinetics law, similarly to the trend of the variation of volume during gel shrinking.

1. Introduction

Phenylene−vinylene conducting polymers (PPV) find applications in luminescent, photovoltaic, electrochromic, and sensory devices.[1,2] The processability of soluble PPV derivatives facilitates the easy fabrication of such electronic devices. Concretely, poly[2-methoxy-5-(3′,7′-dimethyloctyloxy)-1,4-phenylene−vinylene] (MDMO−PPV) presents properties similar to those of the well-established orange-red emitter MEH-PPV, but its processability and film-forming properties are superior.[3]

The factors affecting charge injection and/or doping processes are of great interest for the improvement of the organoelectronic devices fabricated with these polymers.[4,5] Information about the effect of charge injection on physicochemical properties can be studied by spectroscopic methods coupled to a system for the electric control of the conductive polymers.[6−8] Polarons formed upon charge injection produces modifications on the electronic structure of PPV polymers producing photoluminescence quenching.[9,10] In situ electrochemical fluorescence spectroscopy has been successfully applied to the determination of charge transport properties and degradation mechanism in conjugated polyfluorenes.[11] The deactivation of the fluorescence upon polaron-exciton collision was proposed for the explanation of the electrochemical Stern−Volmer kinetics. The relative mobility of charge carriers and the mechanism of electrodegradation have been also determined with this method.[12]

A detailed electrochemical and spectroelectrochemical study of the properties of MDMO−PPV have been performed by in situ electrochemical steady-state fluorescence spectroscopy. Cyclic voltammetry and chronoamperometric studies were performed for the study of electrochemical doping and degradation processes. Potential-dependent emission intensity and scan rate analyses of the fluorescence quenching were used for the determination of the properties of the model polymer.

2. Experimental Section

MDMO−PPV was purchased from Aldrich, and 10 μL of a solution of polymer (1 mg/mL in THF) was spread over 1 cm^2 of indium−tin oxide (ITO) conductive glass (60 Ω^{-1} cm). The solvent for electrochemical measurements was acetonitrile (Merck, HPLC grade), and tetrabutylammonium tetrafluoroborate (Aldrich 99%) was used as supporting electrolyte. The working electrode was a transparent ITO-glass electrode covered with the polymer. The reference electrode was an Ag/AgCl electrode (3 M KCl, Crison) for the conventional electrochemical cell and a silver wire as pseudoreference electrode for the spectroelectrochemical cell, immersed in the same electrolytic solution. A platinum wire was used as auxiliary electrode. Spectroelectrochemical measurements (in situ fluorescence) were performed in a modified fluorescence cell (1-cm-length quartz cell). Details on the cell design were shown in a previous paper.[11] The oxygen was purged from the electrochemical cells by bubbling an argon flow for 20 min, and the argon atmosphere was maintained during all the experiments. In order to remove the water from the electrolytic solution, a molecular sieve (4 Å, Scharlau) was placed into the cell. Fluorescence spectra were acquired at room-temperature using a PTI QuantaMaster Model QM-62003SE spectrofluorometer. All the spectroelectrochemical experiments were reproduced at least two times. The emission spectra were recorded at $\lambda_{ex} = 467$ nm.

3. Results and Discussion

3.1. Characterization of the Polymer. Figure 1 shows the emission and excitation spectra of the polymer deposited onto an ITO plate. An emission maximum at 586 nm and a well-defined vibronic feature at 625 nm are observable. The shape of the spectrum is independent of the excitation wavelength used. The excitation spectrum shows peaks at 450, 467, 482, and 492 nm corresponding to vibrational transitions.

The cyclic voltammograms of an ITO/PPV electrode in acetonitrile are shown in Figure 2a, where the reversible *p*-doping processes can be observed to occur in the polymer. During the positive scan, an oxidation current appears corresponding to the electrochemical formation of positive polaronic species in the polymer, but no well-defined peak is observed within the positive scan up to 1.00 V. In the reverse scan, a

* Corresponding author. E-mail: r.mallavia@umh.es.

10.1021/jp065070s CCC: $33.50 © 2006 American Chemical Society
Published on Web 11/29/2006

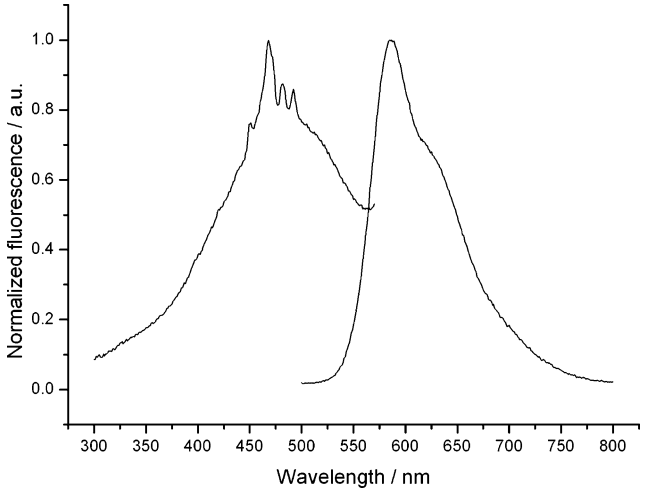

Figure 1. Excitation ($\lambda_{em} = 586$ nm) and emission ($\lambda_{ex} = 467$ nm) spectra of an ITO/PPV electrode.

reduction peak appears at 0.40 V corresponding to the reduction process (dedoping) of the oxidized polymer. The voltammetric charge measured in the forward scan is similar to the charge of the reverse scan, which is indicative of the reversibility of the process. Some differences can be observed in the first and second cycle with respect the stabilized voltammogram (from the fifth cycle). The oxidation onset appears at a higher potential in the first cycle than in the successive scans, and from the fifth cycle, the electrochemical response remains stable. In the stabilized voltammogram, during the positive scan the oxidation current onset is at 0.43V, corresponding to a value of −4.8 eV for the HOMO level. This value is slightly lower than that usually reported for HOMO level of this polymer (−5.3 eV to −5.0 eV).[10,13]

This difference is possibly due to the use of initial voltammograms for the determination of the HOMO level instead of the stabilized one. In fact, the HOMO value would be −5.0 eV if calculated from the onset of the first cycle value. However, we consider more adequate the calculation from the stabilized cycle, since the initial voltammogram may be affected by spurious factors, like contamination of the polymer sample, charge trapping,[14] or first-cycle effects. This well-known phenomenon, called "first-cycle effect" or slow relaxation, has been extensively studied in other polymers, such as polyaniline or poly(*o*-toluidine).[15,16] Several explanations have been given for this phenomenon, as outlined by Mazeikiene and Malinauskas.[17] Structural and morphological changes happening upon electrochemical doping have been proposed in the works by Otero; the polymer doping and swelling have been adjusted to an electrochemically stimulated conformational relaxation model (ESCR).[18,19]

The electrochemical stability was studied by cyclic voltammetry (Figure 2b). In the first scan at potentials higher than 1.10 V (up to 1.85 V), a rising current can be observed from 0.4 V corresponding to the reversible doping of the polymer up to 1.10 V. From that point, a change in the current slope appears corresponding to a second oxidation process with irreversible character. In the second and successive positive scan, lower electrochemical responses are observed, indicating irreversible overoxidation of the polymer.

In order to study the kinetics of the *p*-doping process, a series of chronoamperometric studies were performed. Figure 3 shows the potentiostatic step experiments performed at three different potentials. The presence of a current maximum is more evident at more positive final potentials. This is due to the formation of conductive islands during the polymer oxidation that are characterized by a mechanism of nucleation and ion-diffusion kinetics.[20]

For each chronoamperometric experiment, the representation of the consumed charge (Q) vs $t^{1/2}$ is performed for obtaining the diffusion coefficient of the anion in the polymer. We make use of the Cottrell equation in the form

$$Q = \frac{2zFAC(D^-)^{1/2}}{\pi^{1/2}} t^{1/2} \qquad (1)$$

where z is the charge transferred per anion (BF_4^-) incorporated in the polymer during the oxidation step ($z = 1$), F the Faraday constant, A the geometric area of the electrode, C the concentration of the anion, and D^- its diffusion coefficient. The linear dependence of the charge with $t^{1/2}$ appears in the diffusion-controlled regime. For final potential $E_f = 0.50$ V, the diffusion control appears from 3 s; for $E_f = 0.55$ V, from 10 s; and for $E_f = 0.60$ V, from 30 s. The linear fits are good with regression coefficients $r^2 > 0.999$. Values of D^- were obtained from the three coherent experiments, and its average is $(3.4 \pm 0.3) \times 10^{-12}$ cm^2 s^{-1}. These results are in good agreement with the values of diffusion of tetrafluoroborate anion in other polymers like polytiophene and polypyrrole[21] or poly(ethylene oxide)[22] and is some orders of magnitude lower than that obtained in nanoporous carbons ($\sim 10^{-8}$ cm^2 s^{-1}).[23] Although the Cottrell model is usually employed with planar electrodes, it can be successfully used for the determination of diffusion coefficients in porous polymeric electrodes. The results obtained with this method are comparable to those calculated by ESCR models at low doping levels.[18]

3.2. Spectroelectrochemical Characterization. *3.2.1. In Situ Electrochemical Fluorescence. Electrochemical Quenching and Non-Faradic Relaxation of the Polymer.* The experiments performed by coupling the electrochemical system to the fluorometer are presented in the following section. When the polymer is oxidized, the emission intensity is quenched, similarly to the case of electrochemical quenching of polyfluorene.[11] Figure 4a shows the evolution of the fluorescence emission at 586 nm and the electrode potential as a function of time during nine potential cycles between −0.1 and 0.68 V at 100 mV s^{-1} corresponding to 15.6 s per cycle. Figure 4b represents an equivalent representation of the stable voltammogram and voltafluorogram. At the initial potential of −0.1 V, the fluorescence intensity remains constant, indicating a lack of photobleaching for the polymer in its semiconducting state. As the potential is cycled to more positive values, a sharp decrease of the emission can be observed from 0.4 V in the zone, corresponding to *p*-doping.

The fluorescence decays during the positive-going scan and during the first stages of the reverse scan (where the current is above 0; see Figure 4b) reach a minimum of emission at 0.6 V (in the reverse scan at a potential just before the dedoping peak). The fluorescence starts to rise upon polymer dedoping. However, after the first complete scan (Figure 4a), with the polymer in semiconducting state, the initial fluorescence intensity is not completely restored; only around 70% of the initial emission is reached (Figure 4a). In the second and successive scans, the fluorescence changes similarly with the potential, and a slow descent of the fluorescence of the polymer in semiconducting state can be observed. A stable situation is reached after five complete cycles from 95 s.

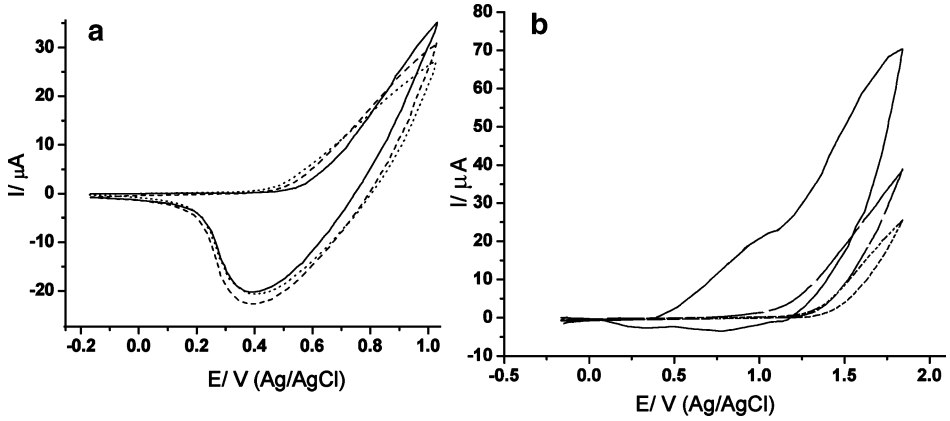

Figure 2. (a) Cyclic voltammogram of the reversible *p*-doping process of ITO/PPV: solid line, first scan; dashed line, second scan; dotted line, fifth scan (stabilized). Scan rate 100 mV s^{-1}. (b) Cyclic voltammogram of the degradation of ITO/PPV: solid line, first scan; dashed line, second scan; dotted line, third scan.

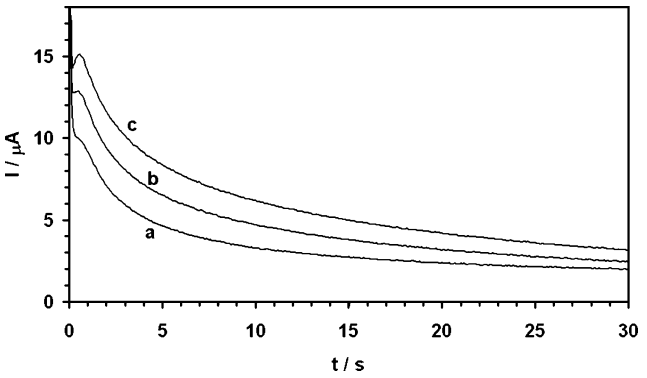

Figure 3. Chronoamperograms obtained during the *p*-doping of an ITO/PPV electrode: initial potential, −0.1 V; final potential, E_f, (a) 0.50 V, (b) 0.55 V, and (c) 0.60 V.

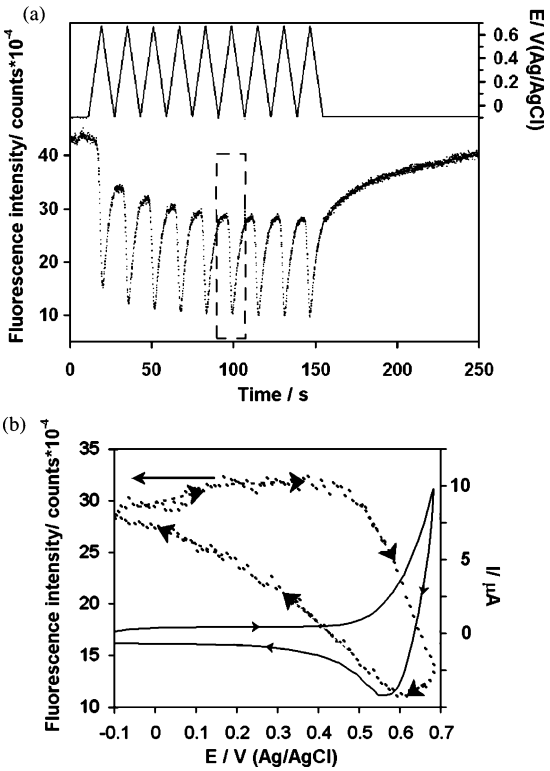

Figure 4. (a) Evolution of the emission intensity (dots) at 586 nm (λ_{ex} = 467 nm) and electrode potential (lines) as a function of time during voltammetric scans between −0.1 and 0.68 V at 100 mV s^{-1}. (b) Stable voltafluorogram (dots) and voltammogram (lines) obtained in the sixth voltammetric scan (inset in Figure 4a)

After the final cycle (t > 157s), the potential is kept at its initial value of −0.1 V. A gradual increasing of the polymer fluorescence intensity can be observed from that point. The initial fluorescence is reached after 350 s in a process that does not involve Faradic current from t > 200s.

In order to study in detail this non-Faradic relaxation process, a series of double potentiostatic step experiments was performed. Figure 5a shows the chronoamperometry and the simultaneous evolution of the fluorescence (chronofluorometry) with the following potential program: −0.1 V → +0.5 V → −0.1 V. The first step arrives to *p*-doping potential, positive current is injected, and the fluorescence decays due to quenching by holes. This potential is kept until the fluorescence reaches a stable minimum. Then the potential is stepped again to −0.1 V. A negative current appears due to electrochemical dedoping. At this point the fluorescence starts to grow rapidly as the polymer is being dedoped, but after 100 s of experiment the current is near zero; therefore, the polymer is dedoped (Figure 5a). The increase of fluorescence in the 100−250 s range can be explained in terms of cathodic shrinking of the polymer, predicted by ESCR models.[18−20] However, the fluorescence is not completely recovered after that time. From $t \approx$ 250 s at −0.1 V, the current is strictly zero, and without Faradic current, the fluorescence grows slowly until reaching its initial value after 1100 s of experiment (Figure 5b).

Morphological modifications are proposed and summarized in the Scheme 1. Initially the fluorescence measured is high, corresponding to the polymer in the semiconducting state, which has low interactions with the solvent. The polymer has a solvatophobic character at this stage. During the first doping step, the strong decrease of the fluorescence corresponds to the quenching of the fluorescence by hole injection and the simultaneous polymer swelling that produces higher interaction with the solvent; the interaction of fluorescent molecules with polar solvents produces the partial deactivation of the emissive states.[24,25]

However, when the polarons are egressed in the reduction step, the fluorescence is not completely recovered. We consider that this lower intensity is due to the different morphology of the dedoped polymer, which is partially swelled. After the complete electrochemical dedoping and cathodic shrinking, we relate the growth of the fluorescence to the non-Faradic shrinking or relaxation of the polymer to its initial state.

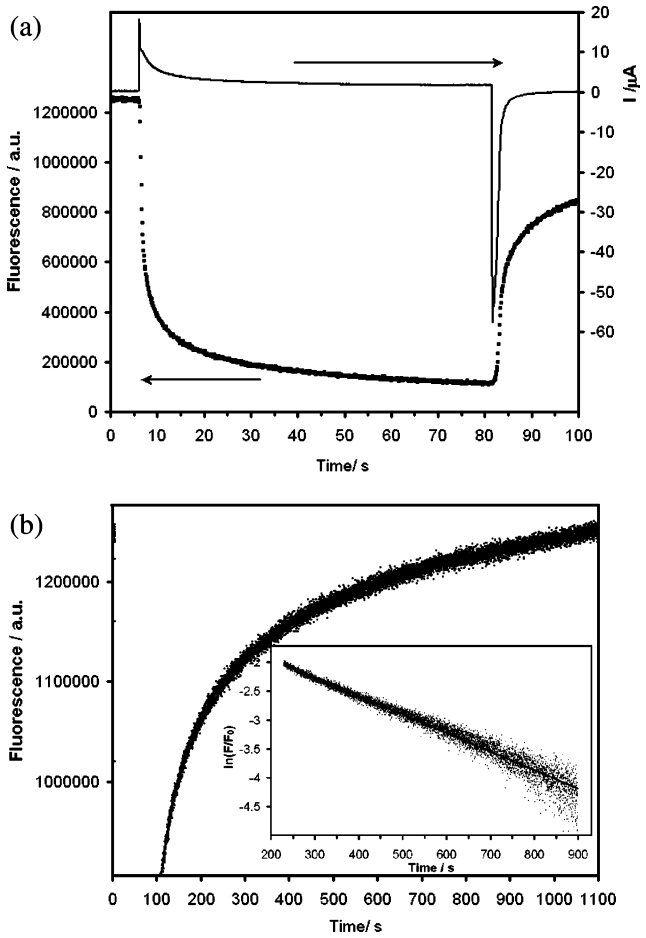

Figure 5. (a) Chronoamperometry (lines) and chronofluorometry (emission 586 nm, dots) of an ITO/PPV electrode. Double potentiostatic step: initial potential, −0.1 V; first step potential, 0.5 V; final potential, −0.1 V. (b) Evolution of the fluorescence emission as a function of time in the non-Faradic process. Inset: representation of $\ln(f/f_0)$ vs time, with f fluorescence emission.

Summarizing, this phenomenon may be explained and modeled in terms of swelling−shrinking of a polymer gel. This process obeys the following first order-kinetics[26]

$$\frac{V(t)}{V(0)} = 1 - B\mathrm{e}^{t/\tau} \tag{2}$$

with $V(t)$ being the volume of the gel at any time (t), $V(0)$ the initial volume of the polymer, B a constant depending on the rheological properties of the gel, and τ a constant inversely proportional to the diffusion coefficient of the solvent. Assuming that during the non-Faradic relaxation of the polymer the variations of fluorescence intensity are proportional to the polymer volume,[27]

$$\ln \frac{f}{f_0} = \ln B' - \frac{t}{\tau'} \tag{3}$$

with f being the fluorescence and f_0 the initial fluorescence of the polymer. The inset of Figure 5b shows plots the logarithmic of the relative fluorescence as a function of the time for the non-Faradic relaxation from 0.5 V and shows a good linear correlation between data.

3.2.2. Kinetic Studies. Electrochemical Stern−Volmer Analyses. The variations of the fluorescence as a function of the injected charge has been successively applied to the study of the charge transport in conjugated polymers making use of

SCHEME 1. Representation of the Morphological Changes Happening upon Electrochemical Doping of the ITO/PPV Electrode

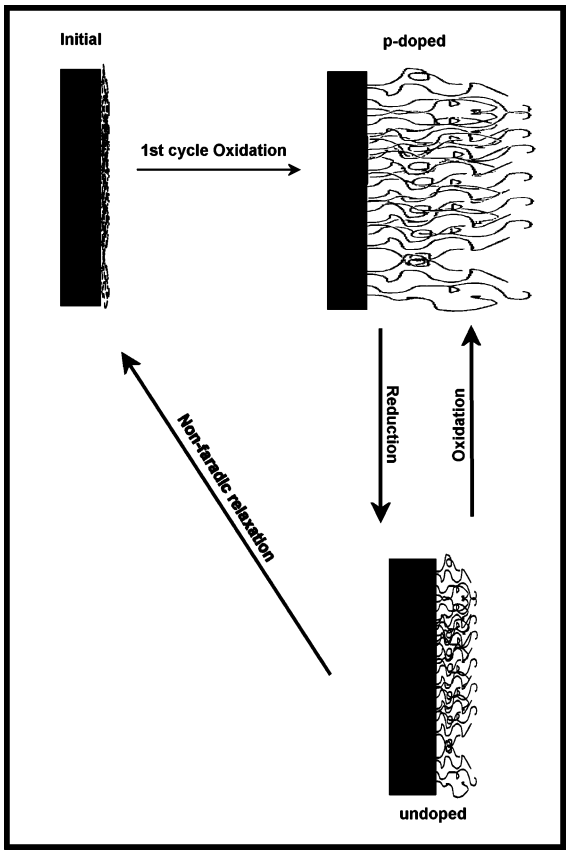

Electrochemical Stern−Volmer plots (ESV plots).[11] Stern−Volmer plots are usually employed to describe collisional quenching of fluorescence, which specifically for electrochemical quenching of conjugated polymers can be expressed as

$$\frac{f_0}{f} = 1 + K_V{}^{+}Q \tag{4}$$

where f_0 and f are the fluorescent emissions in absence and presence of quencher, respectively, Q is the charge injected, and $K_V{}^{+}$ is the ESV constant. The ESV constant is proportional to the diffusion coefficient of the quencher, as expressed by the equation

$$K_V{}^{+} = \Phi D \tag{5}$$

where Φ is a proportionality constant that includes intrinsic parameters of the polymer and D is the apparent diffusion coefficient of the quencher.

The meaning of D in ESV plots of conjugated polymers involves two types of contributions, depending on the experimental conditions employed for the measurement. When the oxidation is performed at high scan rates or in a potentiostatic step, the oxidation process is limited by the diffusion of the ion that compensates the charge injected inside the polymeric matrix. Therefore, D for the oxidation at high scan rates (diffusion-limited) may correspond to the diffusion coefficient of the anion BF_4^- across the polymer. The same experiments performed at low scan rates (charge transfer-limited) will give information about the mobility of the charge.[18] A systematic kinetic study for determining the ESV plot as a function of the potential scan rate, ranging from 0.1 to 1000 mV s^{-1}, has been performed. Figure 6 shows representative electrochemical

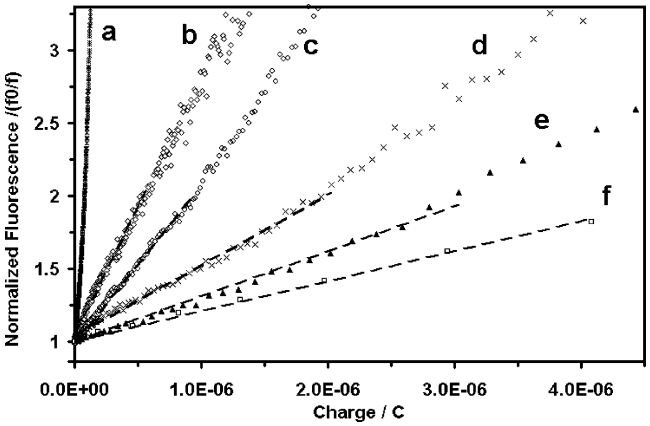

Figure 6. Electrochemical Stern−Volmer (ESV) plots obtained at different scan rates: (a) 1 mV s^{-1}, (b) 5 mV s^{-1}, (c) 10 mV s^{-1}, (d) 20 mV s^{-1}, (e) 50 mV s^{-1}, and (f) 200 mV s^{-1}.

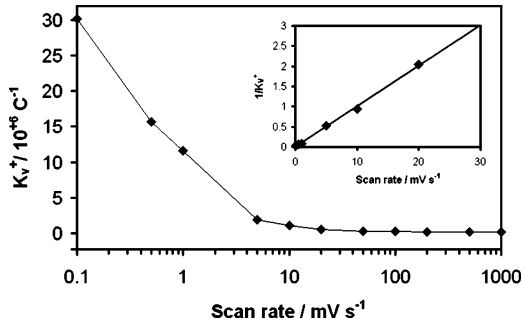

Figure 7. Evolution of the electrochemical Stern−Volmer (ESV) constant, K_V^+, with the potential scan rate (ν). Logarithmic scale is used for clarity. Inset: reciprocal of the K_V^+ vs the scan rate for extrapolation to $\nu = 0$.

Stern−Volmer plots obtained at different scan rates. The fluorescence decay is proportional to the charge injected in the polymer. From the slope of the linear part of the plot the value of the ESV constant K_V^+ can be obtained. As the potential scan rate increases, K_V^+ drops, indicating that the quencher is less efficient at high scan rates.

Figure 7 shows the evolution of the ESV constant as a function of the scan rate. It can be observed that the value of the ESV constant depends on the scan rate. The maximum value is obtained at the lowest scan rate and it decreases as the scan rate rises, reaching a minimum from 200 mV s^{-1}. The value of the scan rate dependent ESV constant can be written as

$$K_V^+(\upsilon) = \Phi D(\upsilon) \tag{6}$$

which is an equivalent expression to eq 5. $D(\upsilon)$ is the apparent diffusion coefficient that depends on the scan rate (υ). For high scan rates the doping process will be controlled by the diffusion of the anion across the polymer network and therefore $D(\upsilon\rightarrow\infty) = D^-$, with D^- being the diffusion coefficient of the tetrafluoroborate anion inside the polymer. For low scan rates, the process is controlled by charge injection and transport of polarons along the polymer, and therefore, $D(\upsilon\rightarrow 0) = D^h$, where D^h is the diffusion coefficient of the charge carriers (positive polarons or holes). The diffusion coefficient can be expressed as mobility by making use of the Einstein equation

$$D^h = \frac{k_B T}{e}\mu_h \tag{7}$$

where e is the charge of the carrier, k_B the Boltzmann constant, and T the temperature.

Taking these limiting conditions,

$$K_V^+(\upsilon\rightarrow 0) = \Phi D^h = \Phi\frac{k_B T}{e}\mu_h \tag{8}$$

$$K_V^+(\upsilon\rightarrow\infty) = \Phi D^- \tag{9}$$

The value for K_V^+ is obtained from the average value for $\nu \geq 200$ mV s^{-1}, which is approximately constant, $K_V^+(\nu\rightarrow\infty) = 2.1 \times 10^5$ C^{-1}. For the extrapolation of K_V^+ to zero, the reciprocal of the constant is represented vs the scan rate (inset in Figure 6b) and the value obtained for $\nu = 0$ is $K_V^+(\nu\rightarrow 0) = 3.8 \times 10^8$ C^{-1}. From the combination of eqs 8 and 9 we can conclude

$$\frac{K_V^+(\upsilon\rightarrow 0)}{K_V^+(\upsilon\rightarrow\infty)} = \frac{k_B T \mu_h}{e\ D^-} \tag{10}$$

Therefore, from the values of the ESV constants, we can estimate the ratio of the diffusion coefficients holes-to-anion. From the experimental results, $K_V^+(\upsilon\rightarrow 0)/K_V^+(\upsilon\rightarrow\infty) = 1800$. In this manner we can calculate the mobility of holes taking the value of diffusion coefficient obtained previously by the Cottrell method. The mobility of holes is $\mu_h = 2.5 \times 10^{-7}$ cm^2 V^{-1} s^{-1}, which is a value in excellent agreement to the values at zero-field reported by Tuladhar et al.[28]

3.3. Conclusions. This work has shown that in situ fluorescence spectroscopy is a valuable and powerful tool for the evaluation of the properties of light-emitting polymers. MDMO−PPV can be electrochemically p-doped in a reversible manner up to 1.10 V. At high potentials, the polymer suffers degradation. Upon electrochemical doping the fluorescence of the polymer is quenched, but the fluorescence is recovered after dedoping. Two effects must be considered in the reactivation of the fluorescence, Faradic reactions (dedoping), and non-Faradic relaxation effects. The change of the fluorescence during non-Faradic relaxation follows a first-order kinetics similarly to the variation of a gel in the course of shrinking.

Kinetic studies of quenching at different potential scan rates were performed by electrochemical Stern−Volmer analyses. The ESV constant K_V^+ measured at high scan rates is proportional to the diffusion coefficient of the anion. K_V^+ at low scan rates is used for the calculation of charge mobility. The diffusion coefficient of tetrafluoroborate across the polymer matrix has been determined by chronoamperometry, using Cottrell's equation.

References and Notes

(1) Schwartz, B. J. *Annu. Rev. Phys. Chem.* **2003**, *54*, 141.
(2) Akcelrud, L. *Prog. Polym. Sci.* **2003**, *28*, 875.
(3) Spreitzer, H.; Becker, H.; Kluge, E.; Kreuder, W.; Schenk, H.; Demandt, R.; Schoo, H. *Adv. Mater.* **1998**, *10*, 1340.
(4) Hoofman, R. J. O. M.; de Haas, M. P.; Siebbeles, L. D. A.; Warman, J. M. *Nature* **1998**, *392*, 54.
(5) Blom, P. W. M.; Vissenberg, M. C. J. M. *Mater. Sci. Eng. R-Rep.* **2000**, *27*, 53.
(6) Damlin, P.; Kvarnstrom, C.; Neugebauer, H.; Ivaska, A. *Synth. Met.* **2001**, *123*, 141.
(7) Damlin, P.; Petr, A.; Kvarnstrom, C.; Dunsch, L.; Ivaska, A. *Synth. Met.* **2001**, *119*, 61.
(8) Gesquiere, A. J.; Park, S. J.; Barbara, P. F. *J. Phys. Chem. B* **2004**, *108*, 10301.
(9) Gesquiere, A. J.; Park, S. J.; Barbara, P. F. *Eur. Polym. J.* **2004**, *40*, 1013.
(10) Holt, A. L.; Leger, J. M.; Carter, S. A. *J. Chem. Phys.* **2005**, *123*.
(11) Montilla, F.; Pastor, I.; Mateo, C. R.; Morallon, E.; Mallavia, R. *J. Phys. Chem. B* **2006**, *110*, 5914.

(12) Montilla, F.; Mallavia, R. On the origin of green emission bands in fluorene-based conjugated polymers. *Adv. Funct. Mater.* In press. (adfm.200600141).
(13) Al Ibrahim, M.; Konkin, A.; Roth, H. K.; Egbe, D. A. M.; Klemm, E.; Zhokhavets, U.; Gobsch, G.; Sensfuss, S. *Thin Solid Films* **2005**, *474*, 201.
(14) Semenikhin, O. A.; Ovsyannikova, E. V.; Ehrenburg, M. R.; Alpatova, N. M.; Kazarinov, V. E. *J. Electroanal. Chem.* **2000**, *494*, 1.
(15) Malinauskas, A.; Bron, M.; Holze, R. *Synth. Met.* **1998**, *92*, 127.
(16) Andrade, E. M.; Molina, F. V.; Florit, M. I.; Posadas, D. *J. Electroanal. Chem.* **1996**, *415*, 153.
(17) Mazeikiene, R.; Malinauskas, A. *Synth. Met.* **2002**, *129*, 61.
(18) Suarez, I. J.; Otero, T. F.; Marquez, M. *J. Phys. Chem. B* **2005**, *109*, 1723.
(19) Grande, H.; Otero, T. F. *J. Phys. Chem. B* **1998**, *102*, 7535.
(20) Otero, T. F.; Grande, H.; Rodriguez, J. *J. Electroanal. Chem.* **1995**, *394*, 211.
(21) Mohammad, F. *Synth. Met.* **1999**, *99*, 149.
(22) Borodin, O.; Smith, G. D.; Douglas, R. *J. Phys. Chem. B* **2003**, *107*, 6824.
(23) Zuleta, M.; Bjornbom, P.; Lundblad, A.; Nurk, G.; Kasuk, H.; Lust, E. *J. Electroanal. Chem.* **2006**, *586*, 247.
(24) Lakowicz, J. R. *Principles of Fluorescence Spectroscopy;* Kluwer Academic/Plenum Publishers: New York, 1999.
(25) Esquembre, R.; Pastor, I.; Mallavia, R.; Mateo, C. R. *J. Photochem. Photobiol. A-Chem.* **2005**, *173*, 384.
(26) Wu, C.; Yan, C. Y. *Macromolecules* **1994**, *27*, 4516.
(27) Pekcan, O., Erdogan, M. *Polym. Int.* **2000**, *49*, 1641.
(28) Tuladhar, S. M.; Poplavskyy, D.; Choulis, S. A.; Durrant, J. R.; Bradley, D. D. C.; Nelson, J. *Adv. Funct. Mater.* **2005**, *15*, 1171.